The Analyst
FULL PAPER

Voltammetric measurements of the interaction of metal complexes with nucleic acids

Mehmet Aslanoglu,*[a] Christian J. Isaac,[b] Andrew Houlton[b] and Benjamin R. Horrocks*[b]

[a] *Department of Chemistry, Harran University, Sanliurfa, Turkey*
[b] *Department of Chemistry, Bedson Building, University of Newcastle upon Tyne, Newcastle upon Tyne, UK NE1 7RU*

Received 6th July 2000, Accepted 16th August 2000
First published as an Advance Article on the web 18th September 2000

Cyclic voltammetry and differential-pulse voltammetry at mm-sized electrodes were used to measure the decrease in the rate of diffusion of metal complexes upon binding to DNA and to extract the binding constants and effective binding site sizes. A linear correlation was observed between the site size determined electrochemically and the diameter of the complexes [site size: $Cu(phen)_2^{2+}$ > $Fe(phen)_3^{2+}$ > $Co(bipy)_3^{3+}$ ≈ $Fe(bipy)_3^{2+}$ > $Ru(NH_3)_6^{3+}$]. The binding constants were found to be influenced by the charge of the metal complex, the nature of ligand and the geometry about the metal centre. Competition experiments, in which differential pulse voltammetry was used to observe the release of bound metal complex on addition of a second DNA-binding molecule to the solution, were sensitive to the nature and location of the binding sites for the two species. Steady-state voltammetric experiments at microelectrodes are shown to have a number of advantages over cyclic voltammetry and differential pulse voltammetry at mm-sized electrodes for determination of binding constants. In particular, the steady-state diffusion limited current is directly proportional to the diffusion coefficient, rather than its square root, which improves the discrimination between DNA-bound and freely diffusing metal complex. Further, the kinetics of the binding process do not affect the steady state measurement, whereas for transient techniques, *e.g.*, cyclic voltammetry, only a range of values can be extracted corresponding to the limits of fast and slow binding kinetics compared to the experimental timescale.

Introduction

The interaction of metal complexes with nucleic acids is of interest for both therapeutic[1–3] and scientific reasons.[4–7] Metal–nucleic acid interactions are responsible for some of the features of nucleic acid structure, in particular magnesium is known to play a role in the stabilisation of RNA and ribosome structures.[6] Chiral ruthenium complexes have been employed as structural probes for different forms and conformations of double stranded DNA.[8–11] Aside from the well-known use of platinum complexes in cancer chemotherapy, metal complex–DNA interactions are also being employed in the development of biosensors. These DNA sensors detect single-stranded DNA using immobilised probe strands of complementary single-stranded DNA. The hybridisation of probe and analyte DNA is detected using the change in the binding affinity for electroactive metal complexes that occurs on hybridisation[12] or by using covalently linked ferrocenyl–oligonucleotide derivatives.[13,14]

Several approaches have been used to measure metal complex–DNA binding including, *e.g.*, luminescence,[15–18] electrophoresis,[19] NMR,[20,21] quartz crystal microgravimetry,[22,23] and electroanalytical techniques.[24–30] The electroanalytical techniques usually rely on the effect of the macromolecule (*e.g.*, DNA) on the diffusion current of the metal complex or other redox active molecule.[24–26] Several workers have shown that binding constants for redox active species can be obtained from straightforward voltammetric experiments in which the DNA is titrated against the redox active molecule. The measurement of diffusion currents in the presence of excess nucleic acid showed that the diffusion coefficient of DNA-bound metal complex (2×10^{-7} cm^2 s^{-1}) was more than one order of magnitude lower than that of the free metal complex.[29] Microelectrodes have also been applied to the measurement of metal cation binding to other polyelectrolytes such as polystyrenesulfonates.[31–33] In this work we report the effect of metal complex charge, geometry and size on the binding parameters. An electrochemical competition technique based on the use of differential pulse voltammetry (DPV) to observe the displacement of bound metal complex by a second DNA-binding molecule, which need not be redox active, is demonstrated. These competition experiments were found to be sensitive to the mode of binding of the metal complex. The binding constants, *K*, and binding site size/base pairs, *s*, are combined with results from competition experiments and previously published work and interpreted in terms of the mode of interaction of the metal complexes with DNA. We also compare steady-state voltammetry at microelectrodes with conventional voltammetry at mm-sized electrodes for the determination of metal complex–DNA binding constants. The data analysis of the microelectrode experiments is shown to be simpler and more precise than for other voltammetric methods due to the reduced contribution of bound metal species to the current. It is also free from assumptions about the kinetics of binding.

Experimental

Materials and instrumentation

Platinum microdisc electrodes were prepared by sealing 25 μm or 10 μm diameter Pt wire (Goodfellow, Cambridge, UK) in 2 mm od glass tubes. Electrical contact to the Pt was made *via* In/Ga eutectic and copper wire. Macroscopic Pt and Au electrodes were prepared by potting 1 mm diameter wires in epoxy. A silver wire was used as a quasi-reference electrode and a tungsten wire as counter electrode. An EG&G Model 263A

potentiostat (EG&G, Reading, UK) was used for all cyclic voltammetry (CV) and differential pulse voltammetry (DPV) experiments. Some microelectrode (UME) experiments employed an OxSys Micros (Oxford, UK) low current potentiostat.

Preparation of DNA solutions

Buffered solutions of DNA (type XIV from Herring testes, Sigma, St. Louis, MO, USA) were prepared fresh before each experiment using doubly distilled water containing 10 mM NaCl and 10 mM TRIS buffer adjusted to pH 7 with HCl. The concentration of nucleic acid is reported as the concentration of nucleotide phosphate and was determined by UV/VIS spectrophotometry using a value of 6600 M^{-1} cm^{-1} for the absorption coefficient.[34] The purity (freedom from bound protein) was assessed from the ratio of the absorbances at 260 nm and 280 nm.[35] In general, the commercial DNA preparation was found to be free of protein (A_{260nm}/A_{280nm} = 1.9) according to this criterion and no further purification was attempted.

Preparation of metal complexes

Racemic $Fe(bipy)_3^{2+}$, $Fe(phen)_3^{2+}$, $Co(bipy)_3^{3+}$ and $Cu(phen)_2^{2+}$ were prepared by stoichiometric reaction of ferrous, cobaltic or cupric salts with the corresponding ligands and recrystallised from water or water–methanol. $Ru(NH_3)_6Cl_3$ was obtained from Fluorochem Ltd. (Derbyshire, UK). All other reagents were of analytical grade or equivalent and obtained from Aldrich (Milwaukee, WI, USA) or Sigma.

Preparation of Δ and Λ-$Fe(phen)_3^{2+}$ and $Fe(bipy)_3^{2+}$

The method used for resolution of Δ and Λ-$Fe(phen)_3^{2+}$ and $Fe(bipy)_3^{2+}$ enantiomers was that of Dwyer and Gyarfas.[36a,b] Potassium antimonyl-*d*-tartrate (2.5 g, 7.7 mmol, 20 mL) was added *via* a burette to *rac*-$Fe(phen)_3SO_4$ (12.2 mmol) in 100 mL water, yielding a dark red precipitate of Λ-$Fe(phen)_3^{2+}(SbO\cdot C_4H_8O_6)_2\cdot 4H_2O$. The mixture was cooled on ice (5 °C) and filtered. The cold solution was treated immediately with stoichiometric aqueous sodium perchlorate and the resulting red precipitate was found to be 76% optically pure ($[\alpha]_D$ = +1083) Δ-$Fe(phen)_3^{2+}$. The Λ-$Fe(phen)_3^{2+}$–antimonyl tartrate precipitate was redissolved in sodium hydroxide (0.01 M, 50 mL), filtered, and then converted to the perchlorate as for Δ-$Fe(phen)_3^{2+}$ yielding 86% optically pure Λ-$Fe(phen)_3^{2+}$ ($[\alpha]_D$ = −1222). Resolution of Δ and Λ-$Fe(bipy)_3^{2+}$ was analogous, except sodium iodide was required to promote precipitation of the diasteromeric iodide antimonyl tartrate. Fractional precipitation produced the less soluble Δ enantiomer and eventual conversion to the perchlorate salts yielded 97.4% ($[\alpha]_D$ = −4675) and 59% ($[\alpha]_D$ = −2425) optically pure Δ and Λ-$Fe(bipy)_3^{2+}$ respectively. All measurements of optical rotation were made on a conventional polarimeter using a water jacketed cell (T = 18 °C) of pathlength 10 cm, bore 4 mm and minimum volume 2.0 mL. The light source was the sodium D-line, (λ = 589 nm). In the case of measurements in DNA containing solutions, the optical rotation was measured with respect to that due to the DNA itself after allowing the $Fe(phen)_3^{2+}$ or $Fe(bipy)_3^{2+}$ to equilibrate for 24 h.

Procedures

Electrochemical determination of binding constants by voltammetric titration. The procedure for voltammetric titrations was identical for cyclic voltammetry, differential pulse voltammetry and microelectrode experiments. An electrochemical cell with a separate reference electrode compartment was used. A known volume, *ca*. 10 mL, of buffered DNA solution was added to the working electrode compartment and voltammograms were recorded as aliquots of metal complex solution were added. The procedure was then repeated using a buffer solution containing no DNA to generate a current–concentration calibration plot.

Electrochemical competition experiments. The initial step in the competition experiments involved placing 20 mL of the TRIS buffer stock solution in the electrochemical cell, followed by an aliquot of the metal complex being studied. A DPV was run and the peak current was noted. The contents of the cell were then discarded and the procedure repeated, using a DNA solution in place of the TRIS buffer solution. Once the peak current had been obtained, an aliquot of the competing ligand–metal complex was added to the cell, followed by a DPV. This procedure was repeated until no further change in the peak current was observed. From these results, the percentage of metal complex released upon addition of the competing ligand–metal complex could be determined.

Data analysis

The effect of polyelectrolytes on the diffusion of metal cations and complexes has been the subject of several papers.[19,24,28–33,37,38] In order to quantify the binding of electroactive metal complexes to DNA, two factors need to be considered. First, a binding model must be chosen in order to relate the concentrations of free and DNA-bound complex in bulk solution to the binding constant and binding site size. Second, voltammetric equations relating the measured current to mass transfer of the mixture of free and bound metal and their concentrations must be chosen. This choice depends on whether the exchange of free and bound species is slow or fast on the timescale of the voltammetric experiment. The binding equilibrium in each case is referred to as 'static' or 'mobile', respectively, in this report.

Modelling the binding equilibrium. The simplest model of the binding of metal complexes to DNA assumes a metal complex–DNA binding equilibrium with a fixed number of non-overlapping binding sites of identical affinity on a given length of DNA. This is equivalent to the well-known Scatchard treatment of binding equilibria.[39] This model has previously been found adequate to fit the experimental data by several workers and was therefore also employed in this work for purposes of comparison. However, the Scatchard treatment is not strictly applicable to DNA since it assumes distinct, non-overlapping binding sites. This assumption is not made in the treatment of the binding by McGhee and von Hippel,[40] which is more complex, but does not contain any extra free parameters.

If the concentration of DNA is expressed in terms of nucleotide phosphate concentration, [NP], and C_b and C_f are the concentrations of free and DNA-bound species respectively, then the Scatchard model binding constant K is given by:

$$K = \frac{C_b}{C_f \dfrac{[NP]}{2s}} \quad (1)$$

where [NP] is the concentration of free nucleotide phosphates and s is the size of the binding site in base pairs. Using the mass balance equations for the total concentration of nucleotide phosphate, $[NP]_0$, this can be expressed in terms of experimentally measureable quantities:

$$\frac{C_b}{C_f} = \frac{[NP]_0}{2s} K(1 - sv) \quad (2)$$

where v is the binding density (*i.e.*, the number of moles of bound metal per mole of total base pairs). The treatment of McGhee and von Hippel takes account of the overlap between binding sites since any contiguous sequence of s unoccupied base pairs may bind a metal complex. The result is an extra combinatorial factor which accounts for the probability that a free base pair has $(s - 1)$ neighbouring base pairs that are also free:

$$\frac{C_b}{C_f} = \frac{[NP]_0}{2s} K(1 - sv)\left[\frac{1 - sv}{1 - (s-1)v}\right]^{s-1} \quad (3)$$

Obtaining the bound and free metal concentrations from voltammetric data. C_f and C_b can be obtained from the diffusion currents in the absence of DNA, i, and in the presence of DNA, i_{dna}:

$$i_{dna} = BD_b^x C_b + BD_f^x C_f \quad (4)$$

$$i = BD_f^x C_T \quad (5)$$

Where B is the appropriate collection of constants for the experiment (electrode area, or radius, sweep rate, *etc.*) and x = 0.5 for cyclic voltammetry or differential pulse voltammetry and x = 1 for a steady-state microdisc experiment. D_f and D_b are the diffusion coefficients of the bound and free metal complex. It should be noted that eqn. (4) assumes that the kinetics of the equilibrium are slow on the cyclic voltammetric timescale. For mobile equilibria eqn. (4) should be replaced by:[41]

$$i_{dna} = BC_T\left(D_b \frac{C_b}{C_T} + D_f \frac{C_f}{C_T}\right)^x \quad (6)$$

For steady state voltammetry at a microdisc x = 1 and as is well known eqn. (6) reduces to eqn. (4). Estimation of K and s from the measured currents (i_{dna} and i) in eqns. (4), (5) and (6) requires the choice of a regression model. Several possible choices have been suggested.[37,42–44] In this work we have computed C_b/C_f and obtained K and s by least squares regression of C_b/C_f on C_T. Using $C_T = C_f + C_b$ we obtain:

$$\frac{D_f^x(i - i_{dna})}{D_f^x i_{dna} - D_b^x i} = \frac{C_b}{C_f} \quad (7)$$

Since $D_f/D_b \approx 50$ we can make the approximation $D_b \ll D_f$ and the left-hand side of eqn. (7) reduces to:

$$\frac{i - i_{dna}}{i_{dna}} = \frac{C_b}{C_f} \quad (8)$$

This expression is accurate to within 2% except at very low metal : DNA ratios where C_f is small. Similarly for a mobile equilibrium with x = 0.5:

$$\frac{i^2 - i_{dna}^2}{i_{dna}^2} = \frac{C_b}{C_f} \quad (9)$$

The left-hand sides of eqns. (8) and (9) can be obtained directly from the experimental diffusion currents. The steady-state data from microelectrode experiments were therefore expressed as plots of $C_b/C_f = (i - i_{dna})/i_{dna}$ against total metal concentration at a fixed concentration of DNA and K and s were obtained by least squares fitting. Non-steady state techniques for which x = 0.5 were plotted according to both eqns. (8), the limit appropriate for a static binding equilibrium, and (9) the limit of mobile equilibrium. The error introduced by the assumption $D_b \ll D_f$ is larger in this case since the ratio $(D_f/D_b)^{0.5}$ is only about 7.[29] A more accurate treatment would require an independent measurement of D_b or the inclusion of D_b as an extra free parameter in the analysis.[24,29] Such a procedure was not carried out in this work since this effect, which is of order 1/7 ($\approx$15%), was within the uncertainty arising from the choice of static or mobile equilibria for our data.

Standard deviations of the fitted parameters were obtained by a bootstrap method which avoids the necessity to make assumptions about the standard deviation and distribution of errors of individual data points other than that they are independent and identically distributed.[45] Briefly, the bootstrap method consists of drawing, with replacement, a random sample of n datapoints from the dataset of n datapoints. This process was repeated to generate 250–1000 simulated data sets and fitted values of the parameters K and s were obtained by the Levenberg–Marquardt method for each data set. This bootstrap sample was used to approximate the sampling distribution of K and s and to compute standard deviations. Bootstrap resampling was performed using software written in-house in MS Fortran 5.1™ incorporating standard routines for non-linear least squares fitting by the Levenberg–Marquardt method.[45] Uncertainties in values of K and s are reported as mean ± standard deviation.

Analysis of electrochemical competition experiments. McGhee and von Hippel's treatment of the binding also includes the case where more than one species competes for binding sites on the same part of the DNA structure. The ratio of bound : free concentrations for any particular species is obtained by summing eqn. (3) over all species, i, as shown in eqn. (10).[40]

$$\frac{C_{ib}}{C_{if}} = \frac{[NP]_0}{2s_i} K_i\left(1 - \sum_i s_i v_i\right)\left[\frac{1 - \sum_i s_i v_i}{1 - \sum_i (s_i - 1)v_i}\right]^{s_i - 1} \quad (10)$$

The subscript i indicates parameters associated with each binding species. This equation describes the binding of one particular species as a function of its free concentration and of the binding of the other species. It can therefore be used to analyse competition experiments, in which the binding of a competing ligand–metal complex is monitored as a function of the concentration of a second metal complex. However, the analysis does not apply when the two species bind to different regions of the DNA double helix, *e.g.*, major and minor grooves. This limits the quantitative aspects of the analysis, but information on the mode of binding can be inferred from a comparison of the experimental competition data with that calculated from eqn. (10) using the binding parameters of the two species determined separately using eqn. (3). Agreement between the experimental data and this formulation suggests that the two species compete for the same regions of DNA, whereas poor agreement is taken as evidence that they bind differently to the DNA.

Results and discussion

Table 1 presents the binding constants and site sizes obtained from differential pulse voltammetry (DPV) experiments in the presence and absence of DNA for the metal complexes: $Fe(bipy)_3^{2+}$, $Fe(phen)_3^{2+}$, $Co(bipy)_3^{3+}$, $Ru(NH_3)_6^{3+}$ and $Cu(phen)_2^{2+}$. In order to facilitate comparison with literature data, the binding parameters from both the treatment of Scatchard [39] and that of McGhee–von Hippel[40] are presented. In addition the analysis was made for both the limiting conditions of static and mobile equilibria. Literature values are shown for comparison, with one exception these values were obtained from a Scatchard-type analysis.

Determination of DNA-binding constants and binding site sizes of metal complexes

Binding of the metal chelates $Fe(bipy)_3^{2+}$, $Fe(phen)_3^{2+}$ and $Co(bipy)_3^{3+}$ to calf thymus DNA has been studied by previous workers using CV and employing a Scatchard-type of binding model.[24] As can be seen from Table 1 our data for *K* and *s* is in reasonable agreement, although there are some differences which may be due to the different sources of DNA and ionic strengths employed. The published binding constant for $Ru(phen)_3^{2+}$ of 6.2×10^3 M^{-1} was determined by equilibrium dialysis utilising the Scatchard analysis.[8] We obtained a similar value for $Fe(phen)_3^{2+}$ from DPV as might be expected for isostructural compounds. Since DNA is a polyanion, electrostatics may be expected to strongly influence the binding.[46–49] However, when other interactions such as hydrophobic effects contribute strongly, it is known that higher oxidation states may in fact bind more weakly. An example is provided by $Co(phen)_3^{2+/3+}$ and $Os(phen)_3^{2+/3+}$.[25,29] At the ionic strengths employed in this work, the charge effect acts simply to increase the binding constant. The effect is much stronger for the bipyridine complexes, which supports the interpretation that these are mainly electrostatic binders. This is consistent with the observation that binding of the $Ru(bipy)_3^{2+}$ complex to DNA is sensitive to millimolar concentrations of monovalent salts, *e.g.*, KCl.[50] In contrast, the ionic strength dependence of the binding of the *tris*(phen) complexes is not as large.[29]

Comparison with the other complexes studied shows $Ru(NH_3)_6^{3+}$ to be one of the strongest DNA binders. Studies of the cobalt analogue, $Co(NH_3)_6^{3+}$ have shown electrostatic interactions are the predominant mode in its DNA interaction, as increasing ionic strength led to a concomitant decrease in the binding constant.[51] However, a more detailed investigation of $Co(NH_3)_6^{3+}$ and various DNAs using ^{59}Co-NMR, presented evidence to suggest a number of distinct classes of DNA-bound $Co(NH_3)_6^{3+}$.[52] It was found that $Co(NH_3)_6^{3+}$ can either: (i) transiently localise, (ii) non-specifically bind but remain highly mobile, or (iii) very tightly locally bind to the DNA helix. The latter, however, only occurs on DNA with a high guanine–cytosine (GC) content, *e.g.*, *M. lysodeikticu* 72% GC. Herring testes DNA used in our study is known to have a GC content of 41%.[53] Therefore, we expect the binding mode of $Ru(NH_3)_6^{3+}$ to be composed of transient localisation and non-specific but highly mobile electrostatic interaction with the DNA helix. Additionally, both $Co(NH_3)_6^{3+}$ and $Ru(NH_3)_6^{3+}$ have been reported as being efficient promoters of the conformational transition of B-DNA to Z-DNA.[54,55] X-ray crystallography of a $Co(NH_3)_6^{3+}$ complex of $(dC\text{-}dG)_3$ has shown that the Z-conformation of the oligonucleotide is stabilised by the presence of five hydrogen bonds formed between the ammonia molecules of the $Co(NH_3)_6^{3+}$ and the phosphate group of the oligonucleotide as well as the N7 and O6 positions of guanine in the major groove. Stabilisation of $Z\text{-}d(CG)_3$ through hydrogen bonding has also been observed for $Ru(NH_3)_6^{3+}$,[56] however, no significant effect on the conformation of calf thymus DNA was observed.[55]

A second important factor determining the binding constant is the number of ligands and coordination geometry around the metal centre. This is apparent by comparison of the Scatchard binding constants for $Fe(phen)_3^{2+}$ and $Cu(phen)_2^{2+}$, which indicates that $Cu(phen)_2^{2+}$ binds *ca.* 12 times more strongly to DNA than $Fe(phen)_3^{2+}$. The formal charge and nature of the ligands on the two complexes are identical; however, by decreasing the number of coordinated phen ligands about the metal centre, a significant increase in binding strength is observed. $Cu(phen)_2^{2+}$ comprises two phen ligands orientated about the copper metal centre in a distorted tetrahedral arrangement.[57] By reducing the number of coordinated phen ligands about the metal centre ($Fe(phen)_3^{2+} \rightarrow Cu(phen)_2^{2+}$) the steric hindrance from the ancillary ligands is reduced, leading to a more substantial overlap of the inserted phen ligand for $Cu(phen)_2^{2+}$ as opposed to the $Fe(phen)_3^{2+}$ case. Studies on the tetrahedral $Zn(phen)_2^{2+}$ and $Zn(phen)Cl_2$ species[58] have also indicated intercalation. Although the groove specificity and binding constants were not reported, it is expected that the binding mode will be similar to that of $Cu(phen)_2^{2+}$.

For both the tris(bipy) complexes, $Co(bipy)_3^{3+}$ and $Fe(bipy)_3^{2+}$ the binding site sizes are ≈ 3.5 base pairs using the McGhee–von Hippel model. However, the tris(phen) complex, $Fe(phen)_3^{2+}$ exhibits a slightly larger binding site size of four base pairs. This probably reflects simply the size of the metal complex and this is supported by the plot of binding site size against the diameter of the metal complex represented by the furthest distance between hydrogen atoms on the ligands in the crystallographic data (Fig. 1). In general, we find that increased charge on the metal complex produces higher binding constants at low ionic strength, but has little influence on the binding site size which is mainly determined by geometric factors.

Comparison of macro- and micro-electrodes for measurement of metal complex–DNA interactions

Fig. 2 shows the effect of the addition of 0.4 mM DNA to a solution of 1.0 mM $Ru(NH_3)_6^{3+}$ on the steady-state microdisc voltammetry of $Ru(NH_3)_6^{3+}$. The current due to reduction of

Table 1 Binding constants and binding site sizes from differential pulse voltammetry

	DPV determination of binding parameters				
Complex	Scatchard (mobile)[a]	Scatchard (static)[a]	McGhee–von Hippel (mobile)[a]	McGhee–von Hippel (static)[a]	Published values
$[Fe(bipy)_3^{2+}]$	$2.2(\pm0.5) \times 10^3$ 4.1(±0.2)	$1.2(\pm0.4) \times 10^3$ 4(±1.7)	$5.8(\pm1.0) \times 10^2$ 3.2(±0.2)	$5.6(\pm1.0) \times 10^2$ 3.5(±0.1)	$1.1(\pm0.6) \times 10^3$ 4.3
$[Fe(phen)_3^{2+}]$	$2.9(\pm0.4) \times 10^4$ 4.4(±.0.08)	$6.9(\pm1.0) \times 10^3$ 3.9(±0.9)	$1.0(\pm0.2) \times 10^4$ 4.2(±0.1)	$9.4(\pm2.4) \times 10^3$ 3.9(±0.1)	$7.1(\pm0.2) \times 10^3$ 5[b]
$[Co(bipy)_3^{3+}]$	$2.0(\pm0.6) \times 10^6$ 5.1(±0.2)	$7.8(\pm1.7) \times 10^3$ 1.1(±0.02)	$1.8(\pm0.9) \times 10^5$ 3.4(±0.5)	$1.8(\pm0.9) \times 10^5$ 3.4(±0.6)	$9.4(\pm1.5) \times 10^3$ 3[b]
$[Ru(NH_3)_6^{3+}]$	$4.3(\pm1.0) \times 10^5$ 2.5(±0.8)	$3.8(\pm0.9) \times 10^4$ 1.9(±1.1)	$4.8(\pm0.3) \times 10^5$ 2.5(±0.03)	$4.9(\pm0.4) \times 10^5$ 2.5(±0.04)	Not applicable
$[Cu(phen)_2^{2+}]$	$2.5(\pm1.8) \times 10^6$ 7(±0.4)	$8.2(\pm2.2) \times 10^4$ 5.3(±0.6)	$2.9(\pm0.7) \times 10^5$ 4.8(±0.3)	$2.3(\pm0.2) \times 10^5$ 4.4(±0.03)	4.7×10^4 2[c]
$[Co(phen)_3^{3+}]$	—	—	—	—	1.6×10^4 6[b]
$[Ru(phen)_3^{2+}]$	—	—	—	—	6.2×10^3 4[b]

[a] Refers to the kinetics of the binding equilibrium. Second figure is *s*. [b] Indicates 50 mM ionic strength. [c] Parameters for $[Cu(phen)_2^{+}]$, measured with 200 mM ionic strength using McGhee–von Hippel method. All other published values cited were analysed using the Scatchard method.

Ru(III) to Ru(II) drops on addition of DNA owing to the strong binding of this trication. To determine the binding constant and binding site size the DNA was titrated with $Ru(NH_3)_6^{3+}$ and the diffusion-limited reduction currents plotted against the total concentration of $Ru(NH_3)_6^{3+}$ (Fig. 3). As can be seen from Fig. 3, at high $[Ru(NH_3)_6^{3+}]$ the current–concentration plots in the presence and absence of DNA ran approximately parallel. The respective values of $Ru(NH_3)_6^{3+}$ diffusion coefficients were 5.0 ± 0.15 × 10^{-6} cm^2 s^{-1} and 5.3 ± 0.1 × 10^{-6} cm^2 s^{-1}. This shows that the decrease in diffusion current on addition of DNA is due to binding of the metal complex and not due to an increased solution viscosity causing a reduction in the diffusion coefficient of $Ru(NH_3)_6^{3+}$. Other workers have reported that the viscosity effect is still negligible at DNA concentrations *ca.* one order of magnitude greater.[24,25] The lower concentration of DNA was used because of the formation of a precipitate at higher concentrations. Fig. 4 shows a plot of $(i - i_{dna})/i_{dna}$ *vs.* C_T for $Ru(NH_3)_6^{3+}$ in the presence of 0.4 mM DNA from steady state microelectrode voltammograms and the corresponding least squares fit to eqn. (2). The binding constant and binding site size obtained were K = 1.47 ± 0.04 × 10^5 M^{-1} and s = 1.62 ± 0.02 base pairs. The value of K was not significantly altered on the inclusion of D_b as another free parameter in the regression analysis and indicates that the error due to the assumption that D_b = 0 made in eqn. (8) is within experimental uncertainties. In contrast, cyclic voltammetric titration of $Ru(NH_3)_6^{3+}$ carried out under identical conditions, with the same data analysis, based on a static binding equilibrium by the Scatchard method, yields a significantly lower value of K as shown in Table 2. This difference between the CV and DPV and microelectrode data is due to the greater contribution of bound metal in the CV and DPV experiments in which current is proportional to $D_b^{1/2}$. The simplified data analysis based on eqn. (8) used in this work is less accurate in the case of CV and DPV because these techniques do not discriminate free and bound metal complex as strongly. This effect is most significant for strongly binding complexes where C_f is low. Correspondingly, in the case of a less strongly bound metal complex, $Fe(bipy)_3^{2+}$, under the same conditions the difference between CV and DPV

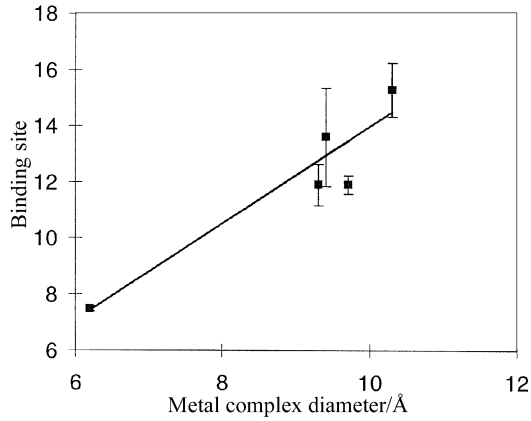

Fig. 1 Binding site size against metal complex diameter. The values are from Table 1 using the McGhee–von Hippel analysis and assuming a mobile equilibrium.

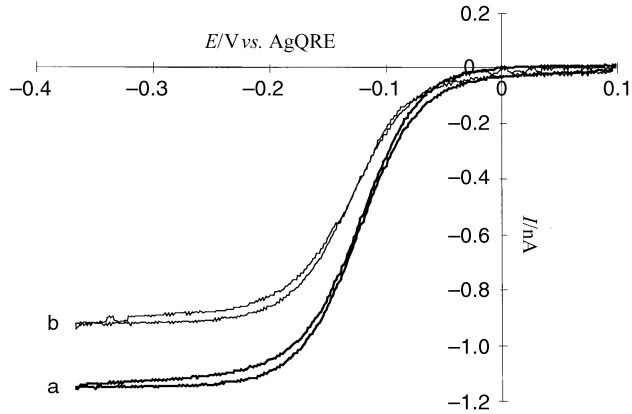

Fig. 2 Steady-state microelectrode voltammograms of 1.0 mM $[Ru(NH_3)_6^{3+}]$ in the (a) absence and (b) presence of 0.4 mM DNA (concentration of nucleotide phosphate). The scan rate was 10 mV s^{-1}, the supporting electrolyte was 10 mM TRIS buffer at pH 7, the reference electrode was a silver wire and the working electrode was a 10 μm diameter Pt disc.

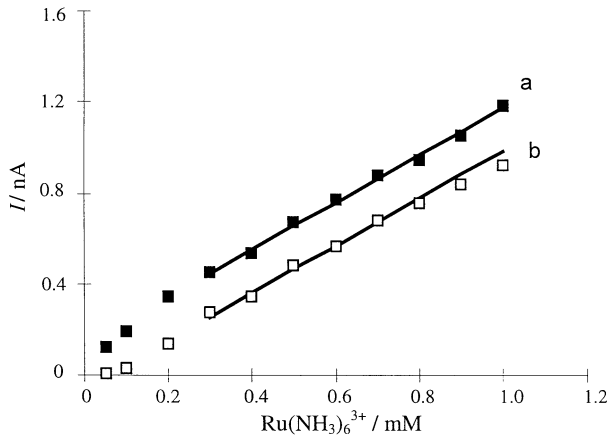

Fig. 3 Plots of steady state diffusion limited current against total concentration of $[Ru(NH_3)_6^{3+}]$ in the (a) absence and (b) presence of 0.4 mM DNA. The scan rate was 10 mV s^{-1}, the supporting electrolyte was 10 mM TRIS buffer at pH 7, the reference electrode was a silver wire and the working electrode was a 10 μm diameter Pt disc. The solid lines are a guide to the eye and indicate the gradient of the plots at high concentrations are roughly equal.

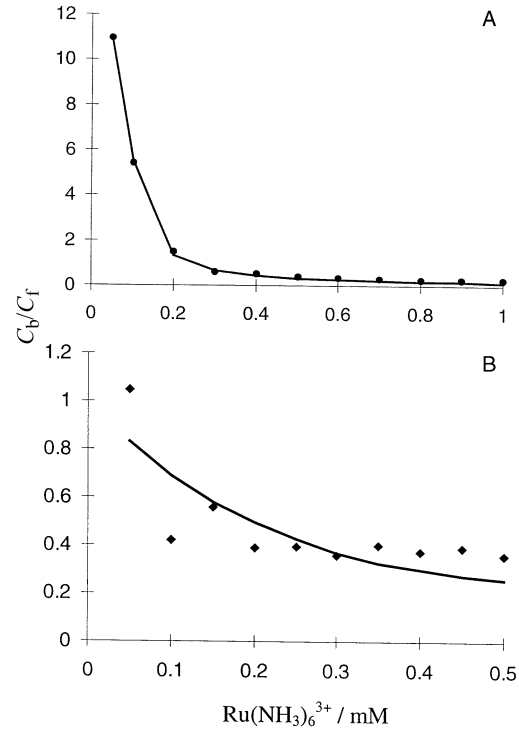

Fig. 4 (A) A plot (symbols) of C_b/C_f *vs.* C_T from the microelectrode titration of $[Ru(NH_3)_6^{3+}]$ against 0.4 mM DNA (concentration of nucleotide phosphate). The ratio of bound to free metal complex was determined from the measured currents in the presence and absence of DNA according to eqn. (7). The solid line shows a least squares fit to the data. The supporting electrolyte was 10 mM TRIS buffer at pH 7, the reference electrode was a silver wire and the working electrode was a 10 μm diameter Pt disc. (B) As (A), but the data was obtained from cyclic voltammetry at a 1 mm diameter Pt disc electrode with a scan rate of 50 mV s^{-1}.

and microelectrode voltammetry was less marked. It should also be noted that the measurement of the current at low $[Ru(NH_3)_6^{3+}]$/[DNA] ratios is easier in the microelectrode experiment than with CV and DPV due to the absence of significant background currents.

Competition experiments

The binding parameters from the McGhee–von Hippel analysis assuming a mobile equilibrium in Table 1 were used to predict the results of competition experiments between pairs of metal complexes and also between metal complexes and *N*-methylphenanthrolinium (MP^+), a classical intercalator for which binding data was available.

Competition between predominantly electrostatic binders. The theoretical analysis based on eqn. (10) and the binding parameters from Table 1, predicts that $Co(bipy)_3^{3+}$ will displace the $Fe(bipy)_3^{2+}$ from the DNA helix. This is in reasonable agreement with the experimental data in Fig. 5 given the uncertainty in the measured binding constants. These results may be interpreted in terms of the counterion condensation theory of Manning and co-workers,[48,59] in which simple cations such as those of the alkali metals, associate with nucleic acids largely as a function of the polymer charge density. A similar mode of association with DNA can be thought of as occurring with the $[M(bipy)_3^{n+}]$ (where M = Co, Fe) complexes. Both $[Co(bipy)_3^{3+}]$ and $[Fe(bipy)_3^{2+}]$ bind to DNA through predominantly electrostatic interactions, with little, if any, ligand interaction appearing to contribute to the overall binding free energy of these complexes. This theory predicts that counterions of high valence 'condense' with the polyelectrolyte, *i.e.*, bind in the region of the sugar–phosphate backbone, whilst lower valence counterions are loosely associated through long range ionic forces in the ionic atmosphere of the polyelectrolyte.

Table 2 A comparison of binding constants and binding site sizes from cyclic voltammetry and steady-state voltammetry at microelectrodes

Complex	Ultramicroelectrode Scatchard	CV Scatchard (static)[a]
$[Fe(bipy)_3^{2+}]$	$1.5(\pm0.2) \times 10^3$	$1.0(\pm0.07) \times 10^3$
	4.1(±0.29)	4.2(±0.09)
$[Fe(phen)_3^{2+}]$	$1.1(\pm0.4) \times 10^4$	$1.4(\pm0.1) \times 10^3$
	4.0(±1.3)	4.0(±0.13)
$[Ru(NH_3)_6^{3+}]$	$1.47(\pm0.04) \times 10^5$	$1.0(\pm0.18) \times 10^4$
	1.62(±0.02)	1.84(±0.03)

[a] Refers to the assumed kinetics of the binding equilibrium.

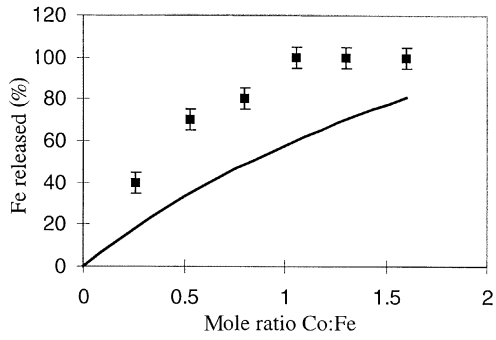

Fig. 5 Percentage of $Fe(bipy)_3^{2+}$ released from DNA on addition of $Co(bipy)_3^{3+}$ *versus* mole ratio of $Co(bipy)_3^{3+}$:$Fe(bipy)_3^{2+}$. The electrode was a 1 mm diameter Pt disc and the solution contained 10 mM TRIS buffer at pH 7 and 10 mM KCl. Differential pulse voltammetry: scan rate 20 mV s^{-1}; pulse height 50 mV; pulse width 50 ms. Symbols are experimental data, the line is theory.

When $Ru(NH_3)_6^{3+}$ is already bound to the DNA helix, similar considerations suggest it will not be displaced by $Fe(bipy)_3^{2+}$ and this was indeed observed, with no more than 4% released even at a mole ratio of 5:1 $Fe(bipy)_3^{2+}$: $Ru(NH_3)_6^{3+}$.

Competition between intercalating complexes. The binding of *rac*-$Fe(phen)_3^{2+}$ to the DNA double helix is composed of two contributions arising from the presence of the two enantiomers Δ and Λ. Equilibration of 0.5 mM Λ, Δ or *rac*-$Fe(phen)_3^{2+}$ with 1.43 mM DNA (by phosphate) results in a mixture which contains a significant excess of Δ-$Fe(phen)_3^{2+}$ (18.9 ± 3.8% at 95% confidence). No significant excess at 95% confidence was observed in the case of the corresponding Λ-$Fe(bipy)_3^{2+}$ complex (2.4 ± 3.2%). Norden and coworkers have also reported experiments in which a CD signal developed on addition of *rac*-$Fe(phen)_3^{2+}$ to DNA with a smaller effect for *rac*-$Fe(bipy)_3^{2+}$.[60] Further, in binding studies on Δ-[$Ru(phen)_3^{2+}$] with DNA, helix lengthening has been observed.[8] A 2D NMR study of Δ-[$Ru(phen)_3^{2+}$] has also observed some nuclear Overhauser effect/enhancement spectroscopy (NOESY) cross peaks between protons on the ligands and on adenine and the sugar unit in the minor groove.[61] These observations suggest that Δ-[$Fe(phen)_3^{2+}$] can partially intercalate one of its phen ligands between the base pairs, while Λ-[$Fe(phen)_3^{2+}$] may bind through electrostatic and van der Waals interactions. Therefore, for a sample of *rac*-[$Fe(phen)_3^{2+}$] binding to DNA, it is expected that a fraction will be loosely bound while the remainder will be partially intercalated, both occurring in the minor groove.

Both the experimental data and theoretical analysis showed that $Cu(phen)_2^{2+}$ and MP^+ compete for the $Fe(phen)_3^{2+}$ binding sites. Although the binding of MP^+ cannot be monitored directly using DPV, the fact that it is competing for the DPV-detectable $Fe(phen)_3^{2+}$ allows the extent of its binding to be indirectly determined. MP^+ is a planar aromatic heterocycle that is known to bind to DNA by intercalation between the base pairs.[62] Consequently, it will have an affinity for similar binding sites on the helix as Δ-$Fe(phen)_3^{2+}$, *i.e.*, between the base pairs. The experimental data shows that in the presence of excess MP^+, approximately 50% of the $Fe(phen)_3^{2+}$ is displaced which is at least consistent with an intercalative binding mode for one enantiomer (Fig. 6).

Competition between electrostatic and intercalative binders. $Ru(NH_3)_6^{3+}$ and MP^+ have different binding modes to DNA. $Ru(NH_3)_6^{3+}$ binds largely through electrostatic association with the negatively charged sugar phosphate backbone, whereas MP^+ intercalates between the base pairs. Since $Ru(NH_3)_6^{3+}$ has a significantly higher binding constant than the other complexes, the McGhee–von Hippel analysis, Fig. 7,

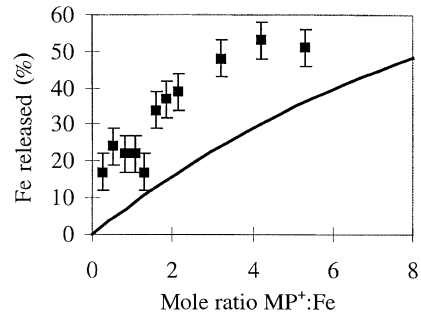

Fig. 6 Percentage of $Fe(phen)_3^{2+}$ released from DNA on addition of MP^+ *versus* mole ratio of MP^+:$Fe(phen)_3^{2+}$. The electrode was a 1 mm diameter Pt disc and the solution contained 10 mM Tris buffer at pH 7 and 10 mM KCl. Differential pulse voltammetry: scan rate 20 mV s^{-1}; pulse height 50 mV pulse width 50 ms. Symbols are experimental data, the line is theory.

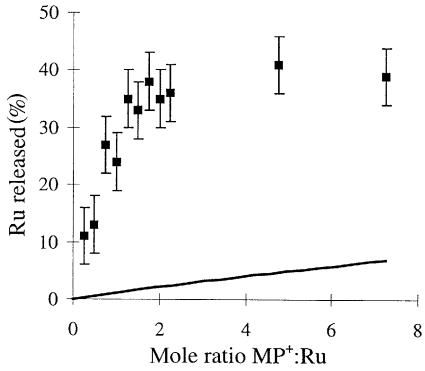

Fig. 7 Percentage of $Ru(NH_3)_6^{3+}$ released from DNA on addition of MP^+ *versus* mole ratio of MP^+:$Ru(NH_3)_6^{3+}$. The electrode was a 1 mm diameter Pt disc and the solution contained 10 mM Tris buffer at pH 7 and 10 mM KCl. Differential pulse voltammetry: scan rate 20 mV s^{-1}; pulse height 50 mV; pulse width 50 ms. Symbols are experimental data, the line is theory.

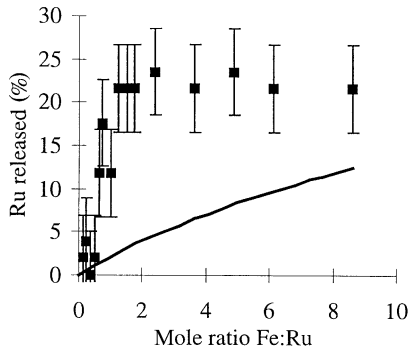

Fig. 8 Percentage of $Ru(NH_3)_6^{3+}$ released from DNA on addition of $Fe(phen)_3^{2+}$ *versus* mole ratio of $Fe(phen)_3^{2+}$:$Ru(NH_3)_6^{3+}$. The electrode was a 1 mm diameter Pt disc and the solution contained 10 mM TRIS buffer at pH 7 and 10 mM KCl. Differential pulse voltammetry: scan rate 20 mV s^{-1}; pulse height 50 mV; pulse width 50 ms. Symbols are experimental data, the line is theory.

predicts no competition of MP^+ against $Ru(NH_3)_6^{3+}$. However, the different binding modes of the two species invalidate the analysis for this system. This is clearly seen in the experimental data which shows that the addition of excess MP^+ to the DNA–$Ru(NH_3)_6^{3+}$ system causes $\approx$40% of the [$Ru(NH_3)_6^{3+}$] to be released from the double helix. The DNA therefore cannot simultaneously accommodate both types of binding, with intercalation favoured over electrostatic binding. This observation may be rationalised by considering the charge density of the DNA double helix. Intercalation of MP^+ will lengthen the double helix and reduce the charge density along the phosphate backbone which decreases the driving force for electrostatic binding.[63] A similar effect is observed (Fig. 8) on addition of *rac*-$Fe(phen)_3^{2+}$ to DNA–$Ru(NH_3)_6^{3+}$ although only $\sim$23% of the $Ru(NH_3)_6^{3+}$ can be displaced. Taken together these experiments provide evidence for an intercalative binding mode for Δ–$Fe(phen)_3^{2+}$.

Conclusions

Steady state voltammetry at ultramicroelectrodes, cyclic voltammetry and differential pulse voltammetry have been used to investigate the interaction of the metal complexes: $Ru(NH_3)_6^{3+}$, $Fe(bipy)_3^{2+}$, $Co(bipy)_3^{3+}$, $Fe(phen)_3^{2+}$ and $Cu(phen)_2^{2+}$ with DNA. The parameters obtained, the binding constant, *K*, and the binding site size, *s*, compare reasonably with previously published values. The binding site size shows a linear correlation with the size of the metal complex. Three main factors influence the binding constant: (i) the charge of the complex, (ii) the nature of the ligands, and (iii) the geometry about the metal centre.

The steady-state voltammetric experiment at microelectrodes was found to have a number of advantages over cyclic voltammetry and differential pulse voltammetry. In particular, the steady-state diffusion limited current is directly proportional to diffusion coefficient, rather than the square root, which improves the discrimination between DNA-bound and freely diffusing metal complex. Further, the kinetics of the binding process do not affect the steady state measurement whereas in the case of transient techniques, *e.g.*, cyclic voltammetry, a range of values is obtained corresponding to the limits of fast and slow binding kinetics compared to the experimental timescale.

For the competition experiments between the electrostatic binding complexes, the experimental data qualitatively fits the theoretical analysis. Similarly, for the competition experiments between the intercalative binding complexes, rough agreement is found. No agreement at all between experimental data and the theoretical analysis is found for the competition between electrostatic and intercalative binding. This confirms that the same binding sites are not involved for the bound and competing complexes. The combination of competition and enantiomeric excess data provides evidence for an intercalation-like mode of binding for Δ-$Fe(phen)_3^{2+}$.

Acknowledgements

Royal Society Small Equipment Grant (BRH) EPSRC, Newcastle University Equipment Fund, Harran University and the Higher Education Council of Turkey.

References

1 B. Rosenberg, L. Van Camp, J. E. Trosko and V. H. Mansour, *Nature*, 1969, **222**, 385.
2 S. J. Lippard, *Acc. Chem. Res.*, 1978, **11**, 211.
3 M. J. Clarke, in *Inorganic Chemistry in Biology and Medicine*, ACS Symposium Series, ed. A. E. Martell, American Chemical Society, Washington, DC, 1980, Vol. 190, p. 157.
4 J. K. Barton, *Prog. Inorg. Chem.*, 1990, **38**, 413.
5 D. H. Johnston, K. C. Glasgow and H. H. Thorp, *J. Am. Chem. Soc.*, 1995, **117**, 8933.
6 G. M. Blackburn and M. J. Gait, *Nucleic Acids in Chemistry and Biology*, IRL Press, New York, 1990.
7 V. A. Bloomfield and I. L. Carpenter, in *Polyelectrolytes; Science and Technology*, ed. M. Hara, Marcel Dekker, New York, USA, 1993, ch. 2 , pp. 77–114 and references cited therein.
8 J. K. Barton, A. T. Denishefsky and J. M. Goldberg, *J. Am. Chem. Soc.*, 1984, **106**, 2172.
9 J. K. Barton, *Comments Inorg. Chem.*, 1985, **3**, 321.
10 J. K. Barton, *Science*, 1986, **233**, 727.
11 C. Stradowski, H. Gorner, L. J. Currell and D. Schulte-Frohlinde, *Biopolymers*, 1987, **26**, 189.
12 K. M. Millan, A. Saurallo and S. R. Mikkelsen, *Anal. Chem.*, 1994, **66**, 2943.
13 S. Takenaka, Y. Uto, H. Kondo, T. Ihara and M. Takagi, *Anal. Biochem.*, 1994, **218**, 436.
14 http://www.microsensor.com
15 M. R. Arkin, E. D. A. Stemp, C. Turro, N. J. Turro and J. K. Barton, *J. Am. Chem. Soc.*, 1996, **118**, 2267.
16 M. Rodriguez and A. J. Bard, *Anal. Chem.*, 1990, **62**, 2658.
17 M. T. Carter and A. J. Bard, *Bioconjugate Chem.*, 1990, **2**, 257.
18 C. V. Kumar, J. K. Barton and N. J. Turro, *J. Am. Chem. Soc.*, 1985, **107**, 5518.
19 A. Z. Li, J. L. Qi, H. H. Shih and K. A. Marx, *Biopolymers*, 1995, **38**, 367.

20 J. P. Rehmann and J. K. Barton, *Biochemistry*, 1990, **29**, 1701.
21 M. L. Bleam, C. F. Anderson and M. T. Record, Jr., *Proc. Natl. Acad. Sci., USA*, 1980, **77**, 3085.
22 X.-H. Xu, H. C. Yang, T. E. Mallouk and A. J. Bard, *J. Am. Chem. Soc.*, 1994, **116**, 8386.
23 H. Su, P. Williams and M. Thompson, *Anal. Chem.*, 1995, **67**, 1010.
24 M. T. Carter, M. Rodriguez and A. J. Bard, *J. Am. Chem. Soc.*, 1989, **111**, 8901.
25 M. T. Carter and A. J. Bard, *J. Am. Chem. Soc.*, 1987, **109**, 7528.
26 J. Swiatek, *J. Coord. Chem.*, 1994, **33**, 191 and references cited therein.
27 C. Price, M. Aslanoglu, C. J. Isaac, M. R. J. Elsegood, W. Clegg, B. R. Horrocks and A. Houlton, *J. Chem. Soc., Dalton Trans.*, 1996, 4115.
28 W. A. Kalsbeck and H. H. Thorp, *Inorg. Chem.*, 1994, **33**, 3427.
29 T. W. Welch and H. H. Thorp, *J. Phys. Chem.*, 1996, **100**, 13 829.
30 D. H. Johnston and H. M. Thorp, *J. Phys. Chem.*, 1996, **100**, 13 837.
31 S. E. Morris, M. Ciszkowska and J. G. Osteryoung, *J. Phys. Chem.*, 1993, **97**, 10 453.
32 M. Ciszkowska and J. G. Osteryoung, *J. Phys. Chem.*, 1994, **98**, 11 791.
33 M. Ciszkowska and J. G. Osteryoung, *J. Phys. Chem.*, 1994, **98**, 3194.
34 M. E. Reichmann, S. A. Rice, C. A. Thomas and P. Doty, *J. Am. Chem. Soc.*, 1954, **76**, 3047.
35 J. Marmur, *J. Mol. Biol.*, 1961, **3**, 208.
36 F. P. Dwyer and E. C. Gyarfas, (*a*) *J. Proc. Roy. Soc. N.S. Wales*, 1949, **83**, 263; (*b*) *J. Proc. Roy. Soc. N.S. Wales*, 1951, **85**, 135.
37 J. L. Garces, F. Mas, J. Cecilia, J. Galceran, J. Salvador and J. Puy, *Analyst*, 1996, **121**, 1855.
38 R. Jiang and F. C. Anson, *J. Phys. Chem.*, 1991, **95**, 5701.
39 G. Scatchard, *Ann. N. Y. Acad. Sci.*, 1949, **51**, 660.
40 J. D. McGhee and P. H. von Hippel, *J. Mol. Biol.*, 1974, **86**, 469.
41 D. H. Evans, *J. Electroanal. Chem.*, 1989, **258**, 451.
42 T. L. Lai and L. Zhang, *Biometrics*, 1994, **50**, 782.
43 P. J. Munson and D. Rodbard, *Anal. Biochem.*, 1980, **107**, 220.
44 R. L. Priore and H. E. Rosenthal, *Anal. Biochem.*, 1976, **70**, 231.
45 W. H. Press, S. A. Teukolsky, W. T. Vetterling and B. P. Flannery, *Numerical Recipes in Fortran*, Cambridge University Press, Cambridge, 2nd edn., 1992, ch. 15.
46 M. C. Olmsted, C. F. Anderson and M. T. Record, Jr., *Proc. Natl. Acad. Sci. USA*, 1989, **86**, 7766.
47 J. Granot, *Biopolymers*, 1983, **22**, 1831.
48 G. S. Manning, *Acc. Chem. Res.*, 1979, **12**, 443.
49 M. T. Record, Jr., C. F. Anderson and T. M. Lohman, *J. Mol. Biol.*, 1976, **107**, 145.
50 C. Stradowski, H. Gorner, L. J. Currell and D. Schulte-Frohlinde, *Biopolymers*, 1987, **26**, 189.
51 G. E. Plum and V. A. Bloomfield, *Biopolymers*, 1988, **27**, 1045.
52 W. H. Braulin and Q. W. Xu, *Biopolymers*, 1992, **32**, 1703.
53 P. Setlow, *Handbook of Biochemistry and Molecular Biology*, 1976, CRC Press, Cleveland, OH, 3rd edn., 1976, vol. 2.
54 R. V. Gessner, G. J. Quigley, A. H. J. Wang, G. A. van der Marel, J. H. van Boom and A. Rich, *Biochemistry*, 1985, **24**, 237.
55 T. J. Thomas and R. P. Messner, *Biochimie*, 1988, **70**, 221.
56 P. S. Ho, C. A. Frederick, D. Saal, A. H. J. Wang and A. Rich, *J. Biomol. Struct. Dyn.*, 1987, **4**, 521.
57 H. Nakai and Y. Deguchi, *Bull. Chem. Soc. Jpn*, 1975, **48**, 2557.
58 J. K. Barton, J. J. Dannenberg and A. L. Raphael, *J. Am. Chem. Soc.*, 1982, **104**, 4967.
59 G. S. Manning, *Q. Rev. Biophys.*, 1978, **11**, 179.
60 T. Hard and B. Norden, *Biopolymers*, 1986, **25**, 1209.
61 M. Ericksson, M. Leijon, C. Hoirt, B. Norden and A. Graslund, *J. Am. Chem. Soc.*, 1992, **114**, 4933.
62 E. J. Gabbay, R. E. Scofield and C. S. Baxter, *J. Am. Chem. Soc.*, 1973, **95**, 7850.
63 M. T. Record, T.M. Lohmann and P. deHaseth, *J. Mol. Biol.*, 1976, **107**, 145.